Microenvironmental immune cell signatures dictate clinical outcomes for PTCL-NOS

杉尾, 健志

REGULAR ARTICLE

blood advances

Microenvironmental immune cell signatures dictate clinical outcomes for PTCL-NOS

Takeshi Sugio,[1] Kohta Miyawaki,[1] Koji Kato,[1] Kensuke Sasaki,[1] Kyohei Yamada,[2] Javeed Iqbal,[3] Toshihiro Miyamoto,[1] Koichi Ohshima,[2] Takahiro Maeda,[4] Hiroaki Miyoshi,[2] and Koichi Akashi[1,4]

[1]Department of Medicine and Biosystemic Science, Graduate School of Medical Sciences, Kyushu University, Fukuoka, Japan; [2]Department of Pathology, School of Medicine, Kurume University, Kurume, Japan; [3]Department of Pathology and Microbiology, University of Nebraska Medical Center, Omaha, NE; and [4]Center for Cellular and Molecular Medicine, Kyushu University Hospital, Fukuoka, Japan

Key Points

- Microenvironmental immune cell signatures stratify PTCL-NOS patients into clinically meaningful disease subtypes.
- Immune-checkpoint inhibitors represent potential therapeutic options for a PTCL-NOS patient subgroup.

Peripheral T-cell lymphoma (PTCL), not otherwise specified (PTCL-NOS) is among the most common disease subtypes of PTCL, one that exhibits heterogeneous clinicopathological features. Although multiple disease-stratification models, including the cell-of-origin or gene-expression profiling methods, have been proposed for this condition, their clinical significance remains unclear. To establish a clinically meaningful stratification model, we analyzed gene-expression signatures of tumors and tumor-infiltrating immune cells using the nCounter system, which enables accurate quantification of low abundance and/or highly fragmented transcripts. To do so, we assessed transcripts of 120 genes related to cancer or immune cells using tumor samples from 68 newly diagnosed PTCL-NOS patients and validated findings by immunofluorescence in tumor sections. We show that gene-expression signatures representing tumor-infiltrating immune cells, but not those of cancerous T cells, dictate patient clinical outcomes. Cases exhibiting both B-cell and dendritic cell (DC) signatures (BD subgroup) showed favorable clinical outcomes, whereas those exhibiting neither B-cell nor DC signatures (non-BD subgroup) showed extremely poor prognosis. Notably, half of the non-BD cases exhibited a macrophage signature, and macrophage infiltration was evident in those cases, as revealed by immunofluorescence. Importantly, tumor-infiltrating macrophages expressed the immune-checkpoint molecules programmed death ligand 1/2 and indoleamine 2, 3-dioxygenase 1 at high levels, suggesting that checkpoint inhibitors could serve as therapeutic options for patients in this subgroup. Our study identifies clinically distinct subgroups of PTCL-NOS and suggests a novel therapeutic strategy for 1 subgroup associated with a poor prognosis. Our data also suggest functional interactions between cancerous T cells and tumor-infiltrating immune cells potentially relevant to PTCL-NOS pathogenesis.

Introduction

Peripheral T-cell lymphoma (PTCL), not otherwise specified (PTCL-NOS) is among the most common subtypes of PTCL. PTCL-NOS does not fit any defined entity of T-cell lymphoma in the World Health Organization (WHO) classification[1] and is often described as belonging to a "wastebasket" category. Prognosis of PTCL-NOS patients is dismal: the 5-year survival rate is as low as 30% due to lack of clinically meaningful disease-stratification models and effective therapies.[2,3] Given PTCL-NOS heterogeneity, identifying molecularly and/or clinically distinct subgroups is necessary to develop novel therapeutic strategies.

Submitted 16 March 2018; accepted 23 July 2018. DOI 10.1182/bloodadvances.2018018754.

The full-text version of this article contains a data supplement.

To classify PTCL-NOS cases, previous studies primarily focused on tumor cells. For example, cell-of-origin (COO) classifications, which define PTCL-NOS cases based on histopathologic features or gene-expression profiles, have been proposed.[4,5] Iqbal et al[4] classified PTCL-NOS cases into 2 subgroups based on expression levels of *TBX21* and *GATA3*, master transcription factors for T helper 1 (Th1) and Th2 development. Similarly, Wang et al[5] demonstrated that high levels of GATA3 protein in tumor cells, as revealed by immunohistochemistry (IHC), are associated with poor prognosis. Although useful, these COO-based methods generally disregard the tumor microenvironment, which could affect multiple facets of tumor pathogenesis, including tumor growth, response to chemotherapy and/or tumor-immune interactions.[6] Given these roadblocks, we set out to establish a novel disease-stratification model based on quantitative measurement of gene-expression signatures derived from both cancerous T cells and the microenvironment. To do so, we used the nCounter system (NanoString Technologies), which enables accurate quantitation of low abundance transcripts in microenvironmental cells. The system also enabled accurate measurement of cross-linked and/or heavily fragmented messenger RNA (mRNA) obtained from formalin-fixed paraffin-embedded (FFPE) samples.[7-10]

Methods

Study population and sample collection

Tumor tissues were extracted from International Peripheral T-Cell and Natural Killer/T-Cell Lymphoma Study cases as well as cases submitted to Kurume University from 2005 to 2011. Pathological diagnosis was made by 2 experienced hematopathologists (H.M. and K.O.) in accordance with the WHO classification.[1] FFPE tumor tissues from 68 PTCL-NOS patients were analyzed.

Clinical data collection and prognostic analysis

Data regarding the observation period and patient survival status were available for 65 cases. The median observation period for survivors was 2.7 years (range, 0.1-11.0 years). Clinical data required to calculate the International Prognostic Index (IPI),[11] including age, Eastern Cooperative Oncology Group (ECOG) performance status (PS), lactate dehydrogenase (LDH) levels, Ann Arbor stage, and the number of extranodal involvement sites, were available in 35 patients. Overall survival (OS) was defined as the time from diagnosis to the last follow-up or death. OS probability was estimated using the Kaplan-Meier method, and statistical significance was determined using the log-rank test in univariate analysis. A Cox proportional hazards model was used to assess predictive values of microenvironmental signatures in multivariate analysis. This study was approved by the institutional ethics committees of Kurume University and the Kyushu University Graduate School of Medical Sciences.

Gene-expression profiling using the nCounter system

RNA was extracted from FFPE samples using the RNeasy FFPE extraction kit (Qiagen, Hilden, Germany) after treatment with deparaffinization solution (Qiagen). Gene-expression levels were assessed using 300 ng of total RNA following the manufacturer's protocol (NanoString Technologies, Seattle, WA). Total RNA was hybridized with gene-specific probes at 65°C for 18 hours, purified and deposited onto a glass cartridge of the nCounter Prep Station using the high-sensitivity protocol. Barcodes uniquely assigned to each target gene were read and counted by a nCounter Digital Analyzer, using the 555 fields of view setting.

The PanCancer immune-profiling panel (NanoString Technologies), which consists of 770 genes related to cancer or immune cells, was used for nCounter-based gene-expression measurements. For data analysis, 114 immune cell–related genes were selected based on the previous reports,[10,12,13] and 6 genes relevant to Th1 (*CXCR3*) or Th2 (*CCR4*, *CCR8*, *PTGDR2*, *IL-4*, and *IL-5*) were also included.[12,13] Normalization of RNA loading was performed using the geometric mean of 40 housekeeping genes included in the panel (supplemental Table 1).

Statistical analysis

The Wilcoxon rank-sum test was used to assess genes differentially expressed between 2 groups. Hierarchical clustering of nCounter data was performed using Ward linkage and Euclidean dissimilarity methods. To assess compactness and distance among clusters in hierarchical clustering analysis, we calculated the Davies-Bouldin Index,[14] which is among the best indices to assess cluster validity.[15] Index values were calculated using the clusterSim package.

Microarray analysis

Microarray data sets of 123 PTCL-NOS or PTCL unspecified cases[4,16] (survival data were available for 63 cases) were obtained from Gene Expression Omnibus (GSE58445 and GSE19069). Quantile normalization of raw data followed by baseline transformation to the median of all samples was performed using GeneSpring 14.5 software (Silicon Genetics, Redwood City, CA). Hierarchical clustering was conducted using Ward linkage and Euclidean dissimilarity methods.

EBV detection

Epstein-Barr virus (EBV) infection was assessed via EBV-encoded RNA (*EBER*) in situ hybridization and/or Southern blot detection of EBV genomes in 57 cases. *EBER* in situ hybridization was performed using a fluorescein-conjugated EBV peptide nucleic acid probe kit (DakoCytomation, Glostrup, Denmark). Southern blot was performed using standard methodologies.

Immunofluorescence

Immunofluorescence was performed on paraffin sections using the Opal multiplex tissue-staining system (PerkinElmer, Waltham, MA). Antibodies used are listed in supplemental Table 2. Antigen retrieval was performed by heating sections to 95°C for 20 minutes in high-pH antigen unmasking solution (H-3301; Vector Laboratories, Burlingame, CA). Slides were visualized using the Mantra quantitative pathology workstation (PerkinElmer). Spatial distribution of $CD3^+$, $CD20^+$, $CD163^+$, or $Langerin^+$ cells and signal intensities of each stain were assessed using inForm (PerkinElmer) and Spotfire (TIBCO, Palo Alto, CA) software.

Results

Microenvironmental immune cell signatures mark PTCL-NOS subgroups

To stratify otherwise heterogeneous PTCL-NOS cases into clinically meaningful subgroups, we analyzed levels of transcripts derived from tumors and microenvironment immune cells. Because standard mRNA expression analysis, such as microarray and RNA sequencing, is not sensitive enough to reliably measure transcripts expressed at low levels in microenvironmental cells, we used the

nCounter system, which enables accurate quantitation of low abundance, highly fragmented transcripts obtained from FFPE samples.[7-10] We obtained RNA samples from 68 newly diagnosed PTCL-NOS cases and analyzed mRNA levels of 120 genes representing 14 immune cell types, including B-cell, dendritic cell (DC), mast cell, neutrophil, eosinophil, macrophage, natural killer (NK)-cell, and T-cell subtypes (Th1, Th2, Th17, follicular helper T-cell [Tfh], γ δ T-cell [Tgd], memory T-cell [Tm], and $CD8^+$ T cell) (Figure 1A; supplemental Table 3).[12,13] Sample quality was assessed by mRNA levels of 40 housekeeping genes in each sample (supplemental Figure 1A). We used the Pearson-correlation matrix followed by hierarchical clustering to assess coexpression patterns of genes related to microenvironmental immune cells and cancerous T cells (Figure 1A-B). Three distinct clusters representing B cells, macrophages, and DCs/mast cells were evident; however, no cluster was evident among T-cell–related genes (Figure 1B). These data indicate that gene sets for B cells, macrophages, and DCs/mast cells accurately represent each cell type in PTCL tissues, whereas cancerous T cells do not necessarily exhibit the "cell-of-origin" phenotypes.

We next performed hierarchical clustering using a gene set representing each immune cell type and assessed its quality using the Davies-Bouldin Index.[14] Gene sets representing B cells, DCs, mast cells, and macrophages formed distinct clusters (Figure 1C), exhibiting a low Davies-Bouldin Index (Figure 1D), whereas those of T-cell subtypes and NK cells barely formed clusters (Figure 1D; supplemental Figure 1B). These data indicate that microenvironmental immune signatures derived from B cells, DCs, mast cells, or macrophages, but not those from cancerous T cells, delineate distinct subgroups of PTCL-NOS cases. Of note, only B-cell–related genes formed a cluster when hierarchical clustering was performed using all 120 immune cell–related genes (supplemental Figure 1C).

A subset of PTCL-NOS cases reportedly exhibits a Tfh-cell phenotype, demonstrating distinct clinicopathological features.[17,18] Although diagnostic criteria for Tfh-PTCL is still under debate, positivity for at least 2 of the Tfh-cell markers (programmed death 1 [PD-1], CD10, B-cell lymphoma 6 [BCL6], CXCL13, and inducible T-cell costimulator [ICOS]) plus CD4 expression is the minimum criteria for Tfh-PTCL.[1] To determine whether Tfh-PTCL cases exist in our cohort, we performed IHC for CD4, CD10, CXCL13, BCL6, and PD-1 in 38 cases. Although some exhibited relatively high mRNA levels of *BCL6*, *CXCL13*, or *PD-1* by the nCounter system, no case was positive for 2 Tfh markers via IHC, suggesting that there was no Tfh-PTCL case in the present cohort (supplemental Figure 1D).

We next validated our findings using publicly available microarray data sets of 123 PTCL-NOS cases from an independent cohort.[4] As expected, B-cell and macrophage signatures clearly stratified cases into 2 distinct subgroups, whereas those of DCs or mast cells did not (supplemental Figure 2A). When hierarchical clustering was performed based on the expression levels of all genes represented in the microarray, only B-cell–related genes were clustered together, possibly due to detection limitations of microarray analysis (supplemental Figure 2B).

Microenvironmental immune cells are evident in PTCL-NOS tissues

We next performed immunofluorescence (IF) to validate our findings in situ. To do so, we used the Mantra system, which enables quantitative measurements of multiple IF signals across an entire section. We labeled microenvironmental immune cells, including B cells, DCs, and macrophages, using lineage-specific, fluorochrome-conjugated antibodies, and measured signal intensities across a section. As expected, $CD20^+$ B cells were abundant only in cases stratified into the B-cell-signature–rich subgroup by the nCounter system (Figure 2A). Frequencies of B cells relative to $CD3^+$ T-cell lineage cells in a defined area of a section were markedly elevated in B-cell-signature–rich cases (Figure 2B). Similarly, we observed $CD1A^+$ DCs only in cases exhibiting a DC signature (Figure 2C). Furthermore, we readily detected cancer-testis (CT) antigens, implying high tumor immunogenicity in this subgroup (supplemental Figure 3A). Interestingly, mRNA levels of *Langerin*, a marker of Langerhans cells,[19,20] and interleukin 15 (*IL-15*), a Langerhans cell–specific chemokine that reportedly enhances T- and NK-cell function,[21-23] were markedly high in DC signature–rich cases (Figure 2D). Chemokine receptors relevant to T-cell migration in the skin or gut mucosa, including *CCR4*,[24,25] *CCR8*,[26] and *CCR9*,[25,27] and their ligands were also abundant in these cases (supplemental Figure 3B). IF analysis confirmed Langerin positivity in $CD1A^+$ DCs (Figure 2E), and frequencies of Langerhans cells in sections were high in DC signature–positive cases (Figure 2F). Of note, these $Langerin^+$ samples were obtained primarily from skin or gastric mucosa (Figure 2G). As expected, macrophage infiltration was also confirmed by CD163 staining only in macrophage signature–rich cases (Figure 2H-I).

We assessed CD20 positivity in 7 B-cell-signature–rich cases and Langerin positivity in 7 DC signature–rich cases. Infiltration of B cells was evident in all B-cell-signature–rich cases examined, whereas DCs were detected in only 5 of 7 DC signature–rich cases. These data suggest that the nCounter system is superior to IF in detecting signatures of rare microenvironmental cells, such as DCs.

Microenvironmental immune cell signatures dictate PTCL-NOS clinical outcomes

We next asked whether microenvironmental immune cell signatures predict clinical outcomes in our cohort, which comprises 65 patients exhibiting survival data similar to that of a historical control[2,3] (supplemental Figure 4A). Cases exhibiting either the B-cell or DC signature showed significantly better prognosis, whereas those with the mast cell or macrophage signature did not (Figure 3A; supplemental Figure 4B). These findings were consistent regardless of the time period (supplemental Figure 4C). Importantly, the B-cell signature, but not that of macrophages, was associated with better prognosis in an independent disease cohort (Figure 3B).[4,16] Of note, biopsy sites were not predictive of clinical outcomes (supplemental Figure 4D), and B-cell signature was still associated with better prognosis when analysis was limited to the samples obtained from lymph nodes (supplemental Figure 4E).

We next stratified cases into 4 subgroups based on B-cell and DC signatures: (1) B-cell signature only (B-only subgroup, n = 18), (2) DC signature only (DC-only subgroup, n = 13), (3) both B-cell and DC signatures (BD subgroup, n = 7), and (4) cases exhibiting neither B-cell nor DC signatures (non-BD subgroups, n = 30). Strikingly, patients in the BD subgroup showed markedly better prognosis (Figure 3C), whereas those in the non-BD subgroup exhibited dismal prognosis (Figure 3C). When we closely examined clinical courses of patients, we found that non-BD cases were primarily resistant to initial therapy (Figure 3D).

Because the COO-based PTCL-NOS classification reportedly delineated PTCL-NOS subgroups,[4,5,16] we next tested whether nCounter-based measurements of COO-related genes would stratify cases into subgroups in our cohort. To do so, we analyzed mRNA levels

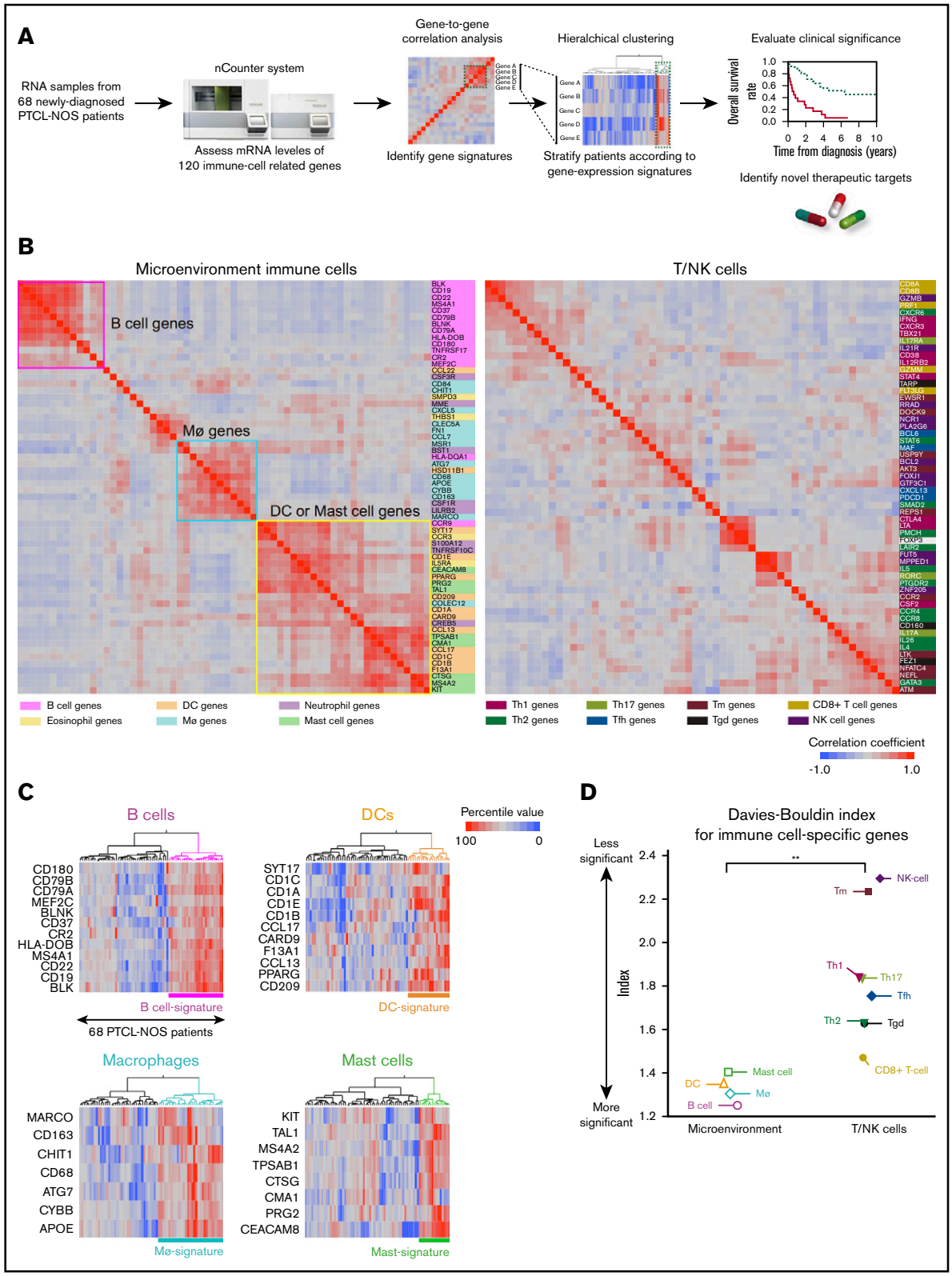

Figure 1. Stratification of PTCL-NOS cases into 4 microenvironmental signatures. (A) Workflow of transcriptomic analysis using the nCounter system. (B) Heat maps show correlation matrix among genes representing microenvironmental immune cells (left) and T/NK cells (right). The correlation matrix was subjected to unsupervised hierarchical clustering. Gene names (right) and corresponding cell-types (bottom) are shown. (C) Hierarchical clustering of 68 PTCL-NOS cases was performed using indicated gene sets. (D) Dot plots represent the Davies-Bouldin Index for each gene set. A gene signature representing a low index score (eg, B cell) serves as a useful classifier. $^{**}P < .01$ (Wilcoxon rank-sum test). Mø, macrophage.

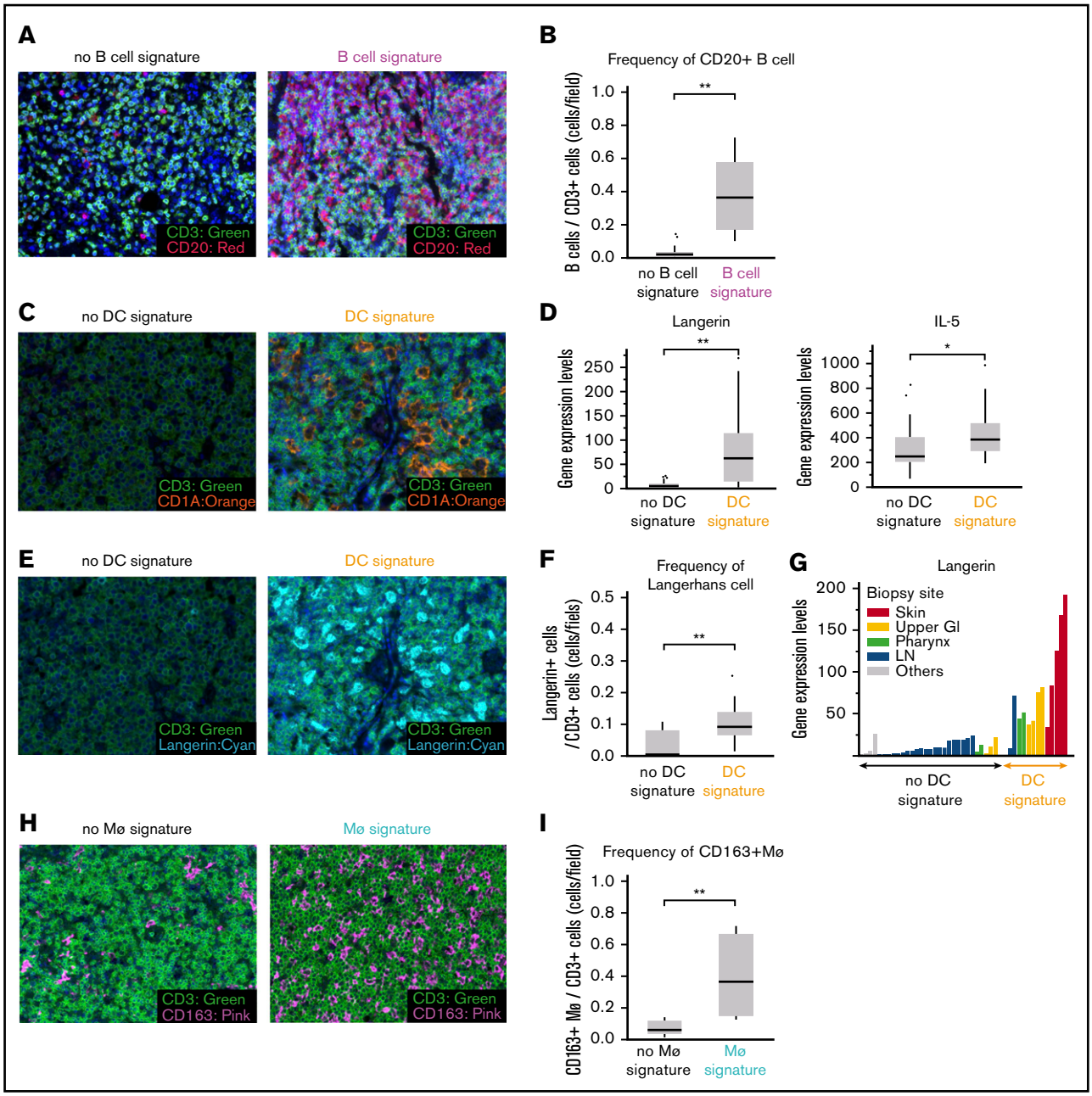

Figure 2. PTCL-NOS tissues harbor microenvironmental immune cells. (A) Representative images of FFPE sections costained with fluorochrome-conjugated anti-CD20 (red) and -CD3 (green) antibodies. Immunofluorescence; original magnification ×20. $CD20^+$ B cells were evident in the B-cell-signature–rich case (right) but not in a case lacking that signature (left). (B) Numbers of $CD20^+$ cells and $CD3^+$ cells were counted across sections using scanning software (see "Methods"). Frequencies of $CD20^+$ cells relative to $CD3^+$ cells are shown. $^{**}P < .01$ (Wilcoxon rank-sum test). (C) Tumor sections were stained with anti-CD1A (orange), a DC marker, and anti-CD3 (green). Representative DC signature–rich (right) and –poor (left) cases are shown. Immunofluorescence; original magnification ×20. (D) Box-and-whisker plots represent *Langerin* (left) and *IL-15* (right) mRNA levels in cases with or without the DC signature. $^{*}P < .05$, $^{**}P < .01$ (Wilcoxon rank-sum test). (E) IF was performed using antibodies against Langerin (cyan), a Langerhans cell marker, and CD3 (green), a T-cell marker. Representative images are shown. Immunofluorescence; original magnification ×20. Langerin expression was evident only in DC signature–rich cases (right). (F) Box-and-whisker plots represent frequencies of DCs as described in panel B. $^{**}P < .01$ (Wilcoxon rank-sum test). (G) Bar graph shows *Langerin* mRNA levels in samples obtained from indicated biopsy sites. (H) IF was performed using antibodies against CD163 (pink), a macrophage marker, and CD3 (green). Representative images are shown. Immunofluorescence; original magnification ×20. (I) Frequencies of $CD163^+$ macrophages relative to $CD3^+$ cells are shown. $^{**}P < .01$ (Wilcoxon rank-sum test).

of Th1, Th2, and cytotoxic T-cell–related genes.[4,5,16] Cases with the Th1-related signature exhibited better clinical outcomes as previously reported (supplemental Figure 5A).[4] In contrast, cytotoxic T-cell–related signature did not provide prognostic values (supplemental Figure 5B).

The IPI[11] is widely used to predict clinical outcomes for non-Hodgkin lymphoma, including PTCL-NOS.[2] Thus, we asked whether microenvironmental immune cell signatures showed prognostic value independent of that of the IPI among 35 patients with available IPI

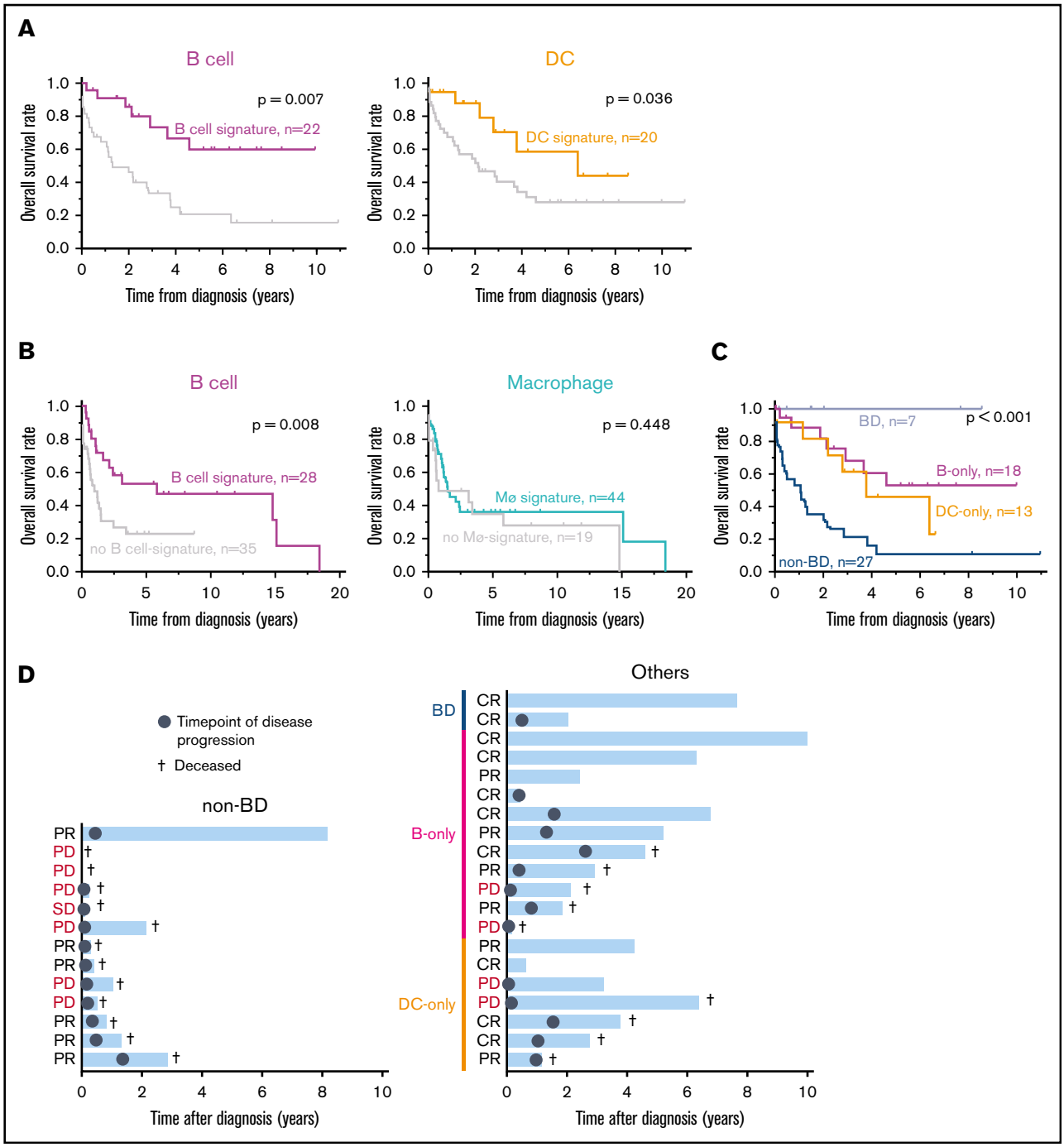

Figure 3. Microenvironmental immune cell signatures dictate clinical outcomes. (A) Kaplan-Meier curves for PTCL-NOS patients with or without B-cell (left) and DC (right) signatures. *P* values were calculated using a log-rank test. (B) Kaplan-Meier curves for 63 PTCL-NOS patients in an independent cohort[4] were generated based on indicated gene signatures. *P* values were calculated using a log-rank test. (C) PTCL-NOS cases were stratified into 4 subgroups according to B-cell and DC signatures, and Kaplan-Meier curves were generated. *P* values were calculated using a log-rank test. (D) Clinical courses of 33 cases. Bar graphs represent survival duration for each patient. Responses to initial therapies are indicated at left. Time of disease progression is depicted as a gray circle. Cases lacking B-cell and DC signatures (non-BD subgroup) were generally resistant to initial therapy (left). B only, only B-cell-signature–positive cases; BD, B-cell– and DC signature–positive cases; CR, complete remission; D only, only DC signature–positive cases; non-BD, cases without B-cell and DC signatures; PD, disease progression; PR, partial remission.

scores (supplemental Table 4). As expected, PS, IPI, and the B-cell signature were highly prognostic in univariate analysis (Table 1). Furthermore, multivariate analysis revealed that B-cell or DC signatures exhibit a prognostic value independent of the IPI (Table 1). EBV positivity was associated with the macrophage signature, but it was not predictive for clinical outcomes (supplemental Figure 6A-B).

Table 1. Univariate and multivariate analysis of 35 patients with available IPI scores

			Univariate analysis			Multivariate analysis	
Variable	**Group**	**n**	**2-y OS, %**	**Median, y**	***P***	**HR, median (95% CI)**	***P***
Age, y	<60	10	50	1.87	.960		
	≥60	25	64	2.92			
Ann Arbor stage	I, II	17	72.5	3.78	.536		
	III, IV	18	50	2.32			
No. of extranodal lesions	0, 1	23	71.9	3.78	.140		
	≥2	12	38.9	1.06			
LDH higher than upper limit	No	20	69.1	3.78	.123		
	Yes	15	48.7	1.32			
Performance status	0, 1	25	82.5	NA	<.001		
	≥2	10	10	0.40			
IPI	Low, Low-int	20	82.9	NA	.006	1.00	.073
	High, High-int	15	33.3	1.06		2.81 (0.91-8.68)	
Sex	Female	10	46.7	1.32	.475		
	Male	25	65.9	3.78			
Initial therapy	CHOP like	26	48.7	1.87	.043	1.00	.485
	Others	9	100.0	NA		0.55 (0.10-2.93)	
B-cell signature	No	20	43.3	1.15	.028	5.52 (1.74-17.5)	.004
	Yes	15	85.1	NA		1.00	
DC signature	No	25	48.9	1.87	.058	8.23 (2.06-32.1)	.003
	Yes	10	88.9	NA		1.00	
Macrophage signature	No	22	69	3.78	.130		
	Yes	13	46.2	1.06			
Mast signature	No	24	51.2	2.84	.376		
	Yes	11	80.8	3.78			

CHOP, cyclophosphamide, doxorubicin, vincristine, and prednisone; CI, confidence interval; HR, hazard ratio; int, intermediate; NA, not applicable.

Tumor-infiltrating macrophages express high levels of immune-checkpoint molecules

Although non-BD cases exhibited an extremely poor prognosis (Figure 3C), we observed that nearly half were also positive for macrophage signature (supplemental Figure 1C). Because immune-checkpoint proteins, whose inhibitors are widely used as anticancer drugs,[28,29] are reportedly expressed on tumor-infiltrating macrophages,[30] we examined levels of programmed death ligand 1 (*PD-L1*), *PD-L2*, and indoleamine 2, 3-dioxygenase 1 (*IDO1*) and found that they were highly expressed in macrophage signature–rich cases (Figure 4A), findings validated in an independent cohort[4,16] (supplemental Figure 7). As expected, PD-L1 and IDO1 proteins were abundant in $CD163^+$ tumor-infiltrating macrophages, as revealed by IF (Figure 4B). Expression of PD-L1 or IDO1 proteins was higher in $CD163^+$ macrophages than in cancerous T cells or other cell types (Figure 4C). mRNA levels of inflammation-related genes (among them, *IFNG* and *GZMB*), which encode proteins that induce *PD-L1* and *IDO1* expression,[31-33] were also high in macrophage-rich cases (Figure 4D).

Discussion

The tumor microenvironment plays a critical role in tumor pathogenesis[12,13] and may impact responses to therapy.[34-36] For example, growth of colorectal cancer cells depends on which cell types infiltrate the tumor microenvironment.[12] In fact, types of tumor-infiltrating immune cells are strong predictors of clinical outcomes across 39 human cancers.[13] In B-cell malignancies, such as follicular lymphoma and diffuse large B-cell lymphoma, microenvironment-based prognostic stratifications have been tested.[34-36] Consistent with this study, the B-cell signature was reportedly associated with favorable prognosis in angioimmunoblastic T-cell lymphoma (AITL).[4,16]

Immune-checkpoint inhibitors, which target interactions between tumor and microenvironmental immune cells, are effective against multiple types of cancers, confirming the significance of microenvironment in cancer therapy.[28,29] In this study, we assessed expression levels of 120 immune cell–related genes and identified a clinically meaningful disease-stratification model for PTCL-NOS based on microenvironmental gene-expression signatures. We also revealed potentially targetable interactions between cancerous T cells and microenvironmental immune cells in a subgroup associated with a poor prognosis (Figure 4E).

Gene-expression signatures of cancerous T cells, the COO-based PTCL-NOS classification, reportedly delineated PTCL-NOS subgroups.[4,5] Patients whose tumor cells expressed high levels of *GATA3*, the master transcription factor for Th2 differentiation,

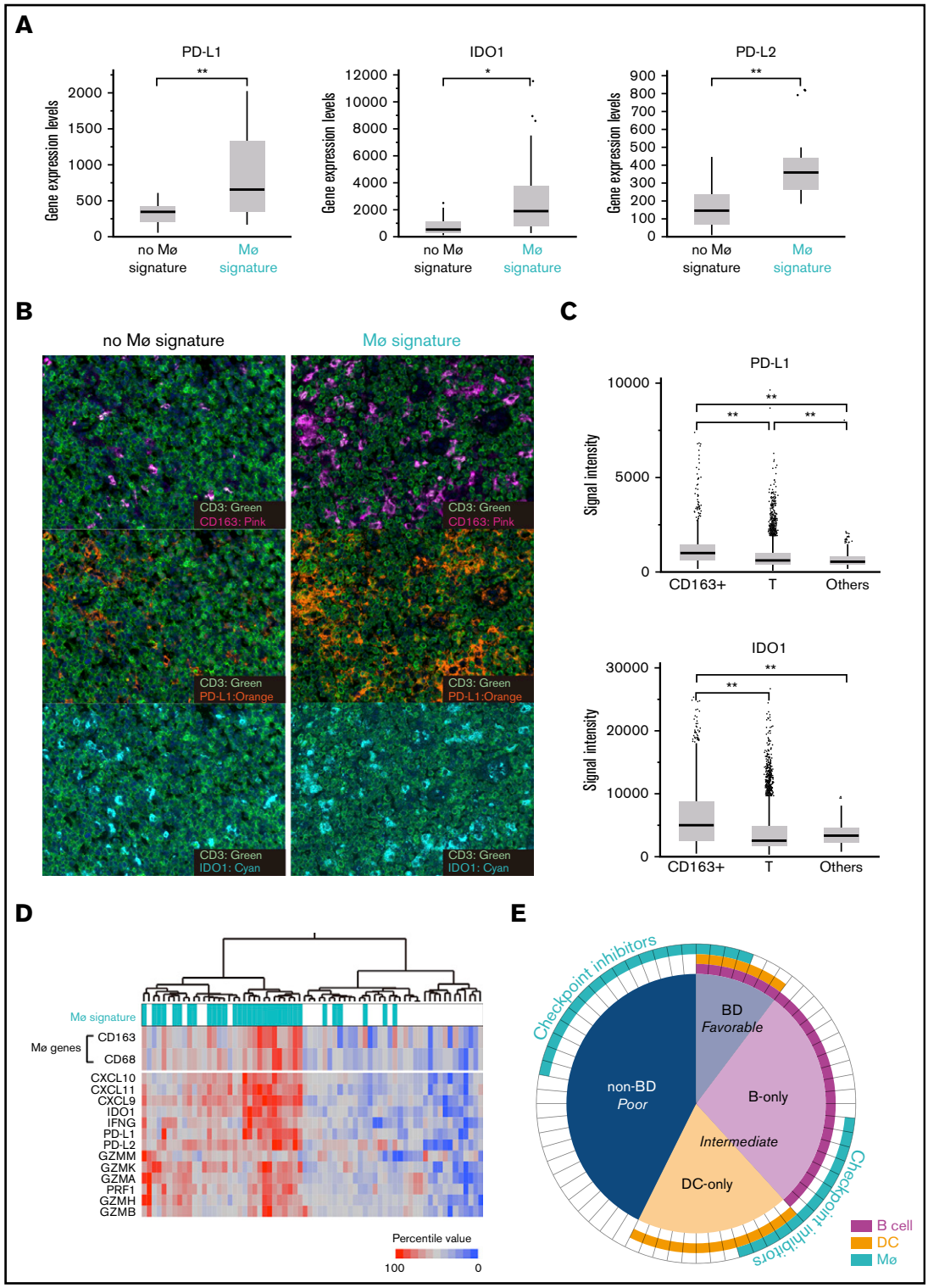

Figure 4. Tumor-infiltrating macrophages express immune-checkpoint molecules. (A) Box-and-whisker plots show *PD-L1*, *IDO1* and *PD-L2* mRNA levels, as revealed by nCounter. *$P < .05$, **$P < .01$ (Wilcoxon rank-sum test). (B) IF was performed using antibodies against CD3 (green, T cells), CD163 (pink, macrophages), PD-L1 (orange), and IDO1 (cyan). Representative images for cases with (right) or without (left) macrophage signatures are shown. Immunofluorescence; original magnification ×20. (C) Box-and-whisker plots represent average signal intensities of PD-L1 (top) or IDO1 (bottom) per cell among indicated cell types. Data were obtained from 3 independent macrophage signature–rich cases. Dots represent outliers. **$P < .01$ (Wilcoxon rank-sum test). (D) Heat map for hierarchical clustering of 68 PTCL-NOS cases based on expression levels of genes related to macrophage and tumor-associated inflammation. (E) Summary of 68 PTCL-NOS cases stratified based on microenvironmental immune cell signatures. Predictive prognostic values and proposed therapy are shown.

exhibited poor prognosis compared with those whose tumors expressed *TBX21*, the Th1 master regulator.[4] *GATA3*-expressing cells coexpressed known *GATA3* target genes (such as *CCR4*, *IL18RA*, *CXCR7*), whereas *TBX21*-expressing cells coexpressed *TBX21* target genes (such as *CXCR3*, *IL2RB*, *CCL3*, *IFNG*).[4] Of note, in concordance with our findings, microenvironmental B-cell signature was associated with favorable prognosis among *TBX21* signature–rich cases.[4] The COO classification stratified our cases into subgroups as previously reported[4]; however, it failed to predict clinical outcomes with statistical significance (supplemental Figure 5). Although reasons for these outcomes are unclear, our cohort may be too small to provide statistical power sufficient for the proposed COO classifications.[4,16]

The COO-based classification primarily assesses characteristics of tumor cells rather than microenvironmental cells. Moreover, few studies have successfully evaluated the microenvironment immune landscape using transcriptome analysis.[12,13] Interrogating tumor-infiltrating immune cells, which comprise a small population in tumors, quantitatively is technically challenging due in part to detection limits of microarray and RNA-sequencing methods. The nCounter system enabled us to quantitatively measure transcript levels in both tumor and microenvironmental cells without polymerase chain reaction (PCR) amplification[8-10] and to detect highly fragmented RNAs in FFPE samples.[7-10] In fact, the nCounter system is currently used to make diagnostic[37,38] and therapeutic[39] decisions in clinical practice. We show here for the first time that it can also be applied to PTCL-NOS, based on our identification of 4 subgroups (BD, B-cell only, DC only and non-BD) that exhibited distinct clinical outcomes (Figure 4E). Immunofluorescence data strongly suggested that the microenvironmental immune cell signatures are not derived from cancerous T cells (Figure 2); however, it is challenging to distinguish normal and malignant T cells in PTCL tissues (eg, normal Th1 vs cancerous T cells with Th1 signature). To do so, clonal T-cell receptor (TCR) rearrangement and/or tumor-specific gene mutation(s) must be assessed at the single-cell level, and the nCounter system is not suitable for these assays.

PTCL-NOS cases exhibiting both B-cell and DC signatures (BD subgroup) responded well to initial therapy and achieved long-term survival (Figure 3C). Reason for this outcome is unclear. In normal secondary lymphoid tissues, B cells and DCs serve as antigen-presenting cells[40] and activate T cells by presenting antigens on major histocompatibility complex molecules and sending costimulatory signals.[41] Thus, PTCL-NOS cells in a B-cell– and DC-rich microenvironment might be more "immunogenic" following chemotherapy-induced tumor lysis.[20,42-44] Tumor-infiltrating DCs were primarily Langerhans cells (Figure 2E), and most DC signature–rich cases were derived from skin or the upper gastrointestinal tract (Figure 2G). Collectively, these data suggest that immunogenicity of cancerous T cells facilitates their clearance by the immune system upon chemotherapy.

In contrast to B-cell– or DC signature–rich cases, cases lacking these signatures, namely, in the non-BD subgroup, exhibited extremely poor prognosis, and almost all patients were refractory to initial therapy (Figure 3C-D). Importantly, macrophages expressing immune-checkpoint molecules, such as PD-L1, PD-L2, and IDO1, were abundant in half of these cases (Figure 4). Considering that tumor-infiltrating T cells induce PD-L1 in solid tumor cells through inflammatory cytokines, namely interferon γ,[31-33] cancerous T cells may induce checkpoint molecules in tumor-infiltrating macrophages. In fact, the macrophage signature was positively associated with the presence of inflammatory cytokine transcripts (Figure 4D).

Taken together, we propose a novel, clinically meaningful disease-stratification model for PTCL-NOS based on microenvironmental gene-expression signatures. We also suggest that immune-checkpoint inhibitors warrant attention as a novel therapeutic strategy for a subset of PTCL-NOS. Because the present cohort is relatively small, larger independent cohorts are needed to validate our stratification model.

Acknowledgments

The authors thank members of the Department of Medicine and Biosystemic Science at Kyushu University for assistance and helpful discussion, and Elise Lamar for critical reading of the manuscript.

This work was supported by Grant-in-Aid for Scientific Research B (16H05340) (T. Miyamoto), Japan Agency for Medical Research and Development (AMED) grants (JP17ck0106163h0002 and JP17cm0106507h0002), Grant-in-Aid for Scientific Research S (16H06391), a Grant-in-Aid for Challenging Exploratory Research (15K15365) (K.A.), Grant-in-Aid for Scientific Research A (17H01567) (T. Maeda), Grant-in-Aid for Scientific Research C (16K09875) (K.K.) and a Grant-in-Aid for Young Scientists (16K19578) (K.M.). This work was also supported by Social Medical Corporation The ChiyuKai Foundation.

Authorship

Contribution: T.S., K.M., H.M., and K.K. coordinated the project; T.S., K.M., K.S., K.Y., and K.K. designed and performed the experiments; T.S., K.M., K.S., K.Y., and H.M., collected clinical information; J.I., H.M., and K.O. provided technical advice; T.S., K.M., H.M., K.K., T. Miyamoto, T. Maeda, and K.A. analyzed and reviewed the data; and T.S., K.M., K.S., and T. Maeda wrote the manuscript with help from all authors.

Conflict-of-interest disclosure: The authors declare no competing financial interests.

ORCID profile: T.S., 0000-0002-4270-1943.

Correspondence: Takahiro Maeda, Center for Cellular and Molecular Medicine, Kyushu University Hospital, 3-1-1 Maidashi, Higashi-ku, Fukuoka 812-8582, Japan; e-mail: t_maeda@cancer.med.kyushu-u.ac.jp; and Hiroaki Miyoshi, Department of Pathology, School of Medicine, Kurume University, 67 Asahimachi, Kurume-city, Fukuoka 830-0011, Japan; e-mail: miyoshi_hiroaki@med.kurume-u.ac.jp.

References

1. Swerdlow SH, Campo E, Harris NL, et al. WHO Classification of Tumours of Haematopoietic and Lymphoid Tissues. Lyon, France: IARC; 2017.
2. Weisenburger DD, Savage KJ, Harris NL, et al; International Peripheral T-Cell Lymphoma Project. Peripheral T-cell lymphoma, not otherwise specified: a report of 340 cases from the International Peripheral T-Cell Lymphoma Project. *Blood*. 2011;117(12):3402-3408.
3. Foss FM, Zinzani PL, Vose JM, Gascoyne RD, Rosen ST, Tobinai K. Peripheral T-cell lymphoma. *Blood*. 2011;117(25):6756-6767.

4. Iqbal J, Wright G, Wang C, et al; Lymphoma Leukemia Molecular Profiling Project and the International Peripheral T-Cell Lymphoma Project. Gene expression signatures delineate biological and prognostic subgroups in peripheral T-cell lymphoma. *Blood*. 2014;123(19):2915-2923.
5. Wang T, Feldman AL, Wada DA, et al. GATA-3 expression identifies a high-risk subset of PTCL, NOS with distinct molecular and clinical features. *Blood*. 2014;123(19):3007-3015.
6. Lenz G, Wright G, Dave SS, et al; Lymphoma/Leukemia Molecular Profiling Project. Stromal gene signatures in large-B-cell lymphomas. *N Engl J Med*. 2008;359(22):2313-2323.
7. Geiss GK, Bumgarner RE, Birditt B, et al. Direct multiplexed measurement of gene expression with color-coded probe pairs. *Nat Biotechnol*. 2008;26(3):317-325.
8. Kojima K, April C, Canasto-Chibuque C, et al. Transcriptome profiling of archived sectioned formalin-fixed paraffin-embedded (AS-FFPE) tissue for disease classification. *PLoS One*. 2014;9(1):e86961.
9. Chen X, Deane NG, Lewis KB, et al. Comparison of nanostring nCounter® data on FFPE colon cancer samples and Affymetrix microarray data on matched frozen tissues. *PLoS One*. 2016;11(5):e0153784.
10. Danaher P, Warren S, Dennis L, et al. Gene expression markers of tumor infiltrating leukocytes. *J Immunother Cancer*. 2017;5:18.
11. International Non-Hodgkin's Lymphoma Prognostic Factors Project. A predictive model for aggressive non-Hodgkin's lymphoma. *N Engl J Med*. 1993;329(14):987-994.
12. Bindea G, Mlecnik B, Tosolini M, et al. Spatiotemporal dynamics of intratumoral immune cells reveal the immune landscape in human cancer. *Immunity*. 2013;39(4):782-795.
13. Gentles AJ, Newman AM, Liu CL, et al. The prognostic landscape of genes and infiltrating immune cells across human cancers. *Nat Med*. 2015;21(8):938-945.
14. Davies DL, Bouldin DW. A cluster separation measure. *IEEE Trans Pattern Anal Mach Intell*. 1979;1(2):224-227.
15. Arbelaitz O, Gurrutxaga I, Muguerza J, Pérez JM, Perona I. An extensive comparative study of cluster validity indices. *Pattern Recognit*. 2013;46(1):243-256.
16. Iqbal J, Weisenburger DD, Greiner TC, et al; International Peripheral T-Cell Lymphoma Project. Molecular signatures to improve diagnosis in peripheral T-cell lymphoma and prognostication in angioimmunoblastic T-cell lymphoma. *Blood*. 2010;115(5):1026-1036.
17. Lemonnier F, Couronné L, Parrens M, et al. Recurrent TET2 mutations in peripheral T-cell lymphomas correlate with TFH-like features and adverse clinical parameters. *Blood*. 2012;120(7):1466-1469.
18. Sakata-Yanagimoto M, Enami T, Yoshida K, et al. Somatic RHOA mutation in angioimmunoblastic T cell lymphoma. *Nat Genet*. 2014;46(2):171-175.
19. Merad M, Ginhoux F, Collin M. Origin, homeostasis and function of Langerhans cells and other langerin-expressing dendritic cells. *Nat Rev Immunol*. 2008;8(12):935-947.
20. Klechevsky E, Morita R, Liu M, et al. Functional specializations of human epidermal Langerhans cells and CD14+ dermal dendritic cells. *Immunity*. 2008;29(3):497-510.
21. Dubois S, Mariner J, Waldmann TA, Tagaya Y. IL-15Ralpha recycles and presents IL-15 in trans to neighboring cells. *Immunity*. 2002;17(5):537-547.
22. Waldmann TA. The biology of interleukin-2 and interleukin-15: implications for cancer therapy and vaccine design. *Nat Rev Immunol*. 2006;6(8):595-601.
23. Mortier E, Woo T, Advincula R, Gozalo S, Ma A. IL-15Ralpha chaperones IL-15 to stable dendritic cell membrane complexes that activate NK cells via trans presentation. *J Exp Med*. 2008;205(5):1213-1225.
24. Reiss Y, Proudfoot AE, Power CA, Campbell JJ, Butcher EC. CC chemokine receptor (CCR)4 and the CCR10 ligand cutaneous T cell-attracting chemokine (CTACK) in lymphocyte trafficking to inflamed skin. *J Exp Med*. 2001;194(10):1541-1547.
25. Mora JR, von Andrian UH. T-cell homing specificity and plasticity: new concepts and future challenges. *Trends Immunol*. 2006;27(5):235-243.
26. Schaerli P, Ebert L, Willimann K, et al. A skin-selective homing mechanism for human immune surveillance T cells. *J Exp Med*. 2004;199(9):1265-1275.
27. Mora JR, Bono MR, Manjunath N, et al. Selective imprinting of gut-homing T cells by Peyer's patch dendritic cells. *Nature*. 2003;424(6944):88-93.
28. Ansell SM, Lesokhin AM, Borrello I, et al. PD-1 blockade with nivolumab in relapsed or refractory Hodgkin's lymphoma. *N Engl J Med*. 2015;372(4):311-319.
29. Topalian SL, Hodi FS, Brahmer JR, et al. Safety, activity, and immune correlates of anti-PD-1 antibody in cancer. *N Engl J Med*. 2012;366(26):2443-2454.
30. Wilcox RA, Feldman AL, Wada DA, et al. B7-H1 (PD-L1, CD274) suppresses host immunity in T-cell lymphoproliferative disorders. *Blood*. 2009;114(10):2149-2158.
31. Abiko K, Matsumura N, Hamanishi J, et al. IFN-γ from lymphocytes induces PD-L1 expression and promotes progression of ovarian cancer. *Br J Cancer*. 2015;112(9):1501-1509.
32. Bellucci R, Martin A, Bommarito D, et al. Interferon-γ-induced activation of JAK1 and JAK2 suppresses tumor cell susceptibility to NK cells through upregulation of PD-L1 expression. *OncoImmunology*. 2015;4(6):e1008824.
33. Spranger S, Spaapen RM, Zha Y, et al. Up-regulation of PD-L1, IDO, and T(regs) in the melanoma tumor microenvironment is driven by CD8(+) T cells. *Sci Transl Med*. 2013;5(200):200ra116.
34. Glas AM, Knoops L, Delahaye L, et al. Gene-expression and immunohistochemical study of specific T-cell subsets and accessory cell types in the transformation and prognosis of follicular lymphoma. *J Clin Oncol*. 2007;25(4):390-398.

35. Lenz G, Wright GW, Emre NCT, et al. Molecular subtypes of diffuse large B-cell lymphoma arise by distinct genetic pathways. *Proc Natl Acad Sci USA*. 2008;105(36):13520-13525.

36. Dave SS, Wright G, Tan B, et al. Prediction of survival in follicular lymphoma based on molecular features of tumor-infiltrating immune cells. *N Engl J Med*. 2004;351(21):2159-2169.

37. Scott DW, Wright GW, Williams PM, et al. Determining cell-of-origin subtypes of diffuse large B-cell lymphoma using gene expression in formalin-fixed paraffin-embedded tissue. *Blood*. 2014;123(8):1214-1217.

38. Ng SWK, Mitchell A, Kennedy JA, et al. A 17-gene stemness score for rapid determination of risk in acute leukaemia. *Nature*. 2016;540(7633):433-437.

39. Wallden B, Storhoff J, Nielsen T, et al. Development and verification of the PAM50-based Prosigna breast cancer gene signature assay. *BMC Med Genomics*. 2015;8(1):54.

40. Hughes CE, Benson RA, Bedaj M, Maffia P. Antigen-presenting cells and antigen presentation in tertiary lymphoid organs. *Front Immunol*. 2016;7(3):481.

41. Chen L, Flies DB. Molecular mechanisms of T cell co-stimulation and co-inhibition [published correction appears in *Nat Rev Immunol*. 2013;13(7):542]. *Nat Rev Immunol*. 2013;13(4):227-242.

42. Engelhardt JJ, Boldajipour B, Beemiller P, et al. Marginating dendritic cells of the tumor microenvironment cross-present tumor antigens and stably engage tumor-specific T cells. *Cancer Cell*. 2012;21(3):402-417.

43. Nielsen JS, Sahota RA, Milne K, et al. CD20+ tumor-infiltrating lymphocytes have an atypical CD27- memory phenotype and together with CD8+ T cells promote favorable prognosis in ovarian cancer. *Clin Cancer Res*. 2012;18(12):3281-3292.

44. Garnelo M, Tan A, Her Z, et al. Interaction between tumour-infiltrating B cells and T cells controls the progression of hepatocellular carcinoma. *Gut*. 2017;66(2):342-351.